

Does the full configuration interaction method based on quantum phase estimation with Trotter decomposition satisfy the size consistency condition?

Kenji Sugisaki^{1,2,3}

¹⁾Graduate School of Science and Technology, Keio University, 7-1 Shinkawasaki, Saiwai-ku, Kawasaki, Kanagawa 212-0032, Japan

²⁾Quantum Computing Center, Keio University, 3-14-1 Hiyoshi, Kohoku-ku, Yokohama, Kanagawa 223-8522, Japan

³⁾Centre for Quantum Engineering, Research and Education, TCG Centres for Research and Education in Science and Technology, Sector V, Salt Lake, Kolkata 700091, India

(*Electronic mail: ksugisaki@keio.jp)

(Dated: 18 June 2024)

Electronic structure calculations of atoms and molecules are expected to be a promising application for quantum computers, and two important algorithms, the quantum phase estimation (QPE) and the variational quantum eigensolver (VQE), have been widely studied. The condition that the energy of the dimer consisting of two monomers separated by a large distance should be twice of the energy of the monomer, known as a size consistency, is very important in quantum chemical calculations. Recently, we reported that the size consistency condition can be broken by the Trotterization in the unitary coupled cluster singles and doubles (UCCSD) ansatz in VQE, when the molecular orbitals delocalized to the dimer are used (K. Sugisaki *et al.*, *J. Comput. Chem.*, published online; DOI: 10.1002/jcc.27438). It is well known that the full configuration interaction (full-CI) energy is invariant with arbitrary rotations of molecular orbitals, and therefore the QPE-based full-CI in principle satisfies the size consistency. However, Trotterization of the time evolution operator has a chance to break the size consistency conditions. In this work, we investigated whether or not the size consistency condition can be maintained by the Trotterization of the time evolution operator in the QPE-based full-CI calculations. Our numerical simulations revealed that the size consistency of the QPE-based full-CI is not automatically violated by using the molecular orbitals delocalized to the dimer, but the use of an appropriate Trotter decomposition condition is crucial to satisfy the size consistency condition. Acceleration of the QPE simulations with sequential addition of ancillary qubits is also reported.

I. INTRODUCTION

Solving the Schrödinger equation of atoms and molecules as accurately as possible is one of the goals of quantum chemistry. The full configuration interaction (full-CI) method is able to give variationally best wave functions and energies within the Hilbert space spanned by the basis set used. However, the computational cost of the full-CI method grows exponentially with the number of basis functions and electrons, and it is impractical except for small molecules with simple basis sets. The possibility of using a quantum computer to solve the full-CI using the quantum phase estimation (QPE) algorithm was proposed in 2005.¹ Since then, a number of theoretical studies on the QPE-based quantum chemical calculations^{2–13} and on the extension of the QPE algorithm^{14–18} have been reported. On the experimental side, iterative QPE-based full-CI/STO-3G calculations of the H₂ molecule have been reported in 2010 with photonic¹⁹ and NMR²⁰ quantum processors, using one qubit for wave function encoding. The same system has been investigated with two qubits for wave function storage, using superconducting qubits in 2016²¹, and on an ion-trap quantum processor in conjunction with a Bayesian QPE framework with quantum error detection.²² The experimental demonstration of the full-CI/STO-3G of the HeH⁺ molecule is also reported using the NV center of the diamond system.²³

In 2014, the quantum–classical hybrid approach known as

a variational quantum eigensolver (VQE) was proposed for the quantum chemical calculations using noisy intermediate-scale quantum (NISQ) devices.^{24,25} In VQE, an approximate wave function is generated on a quantum computer using a parameterized quantum circuit defined by an “ansatz”, and the energy expectation value is computed by statistical sampling of the quantum circuit measurement results. As a physically motivated ansatz, the unitary coupled cluster (UCC) ansatz defined as

$$|\Psi_{\text{UCC}}\rangle = e^{T-T^\dagger} |\Psi_{\text{HF}}\rangle \quad (1)$$

has been widely used.²⁶ Here, $|\Psi_{\text{HF}}\rangle$ is the Hartree–Fock (HF) wave function and T and T^\dagger are excitation and de-excitation operators, respectively, from the HF wave function. The UCC ansatz by considering single and double excitation operators as T , known as the UCCSD ansatz, usually gives accurate correlation energies for typical closed shell molecules.

In quantum chemical calculations, the energy of the dimer consisting of the monomers sufficiently separated from each other should be twice of the energy of the monomer. This condition, known as a size consistency,²⁷ is very important, especially in the calculation of large molecules. The truncated configuration interaction expansions such as CISD and CISDT do not satisfy the size consistency, while the truncated coupled cluster methods like CCSD and CCSDT do. The UCCSD ansatz used in the VQE framework is based on the cluster expansion, and it has been taken for granted that it is size consis-

tent. However, in the VQE, the UCCSD ansatz is usually implemented by using the Trotter decomposition to construct the parameterized quantum circuit. Recently we have numerically demonstrated that the Trotterized UCCSD ansatz does not automatically satisfy the size consistency condition.²⁸ The size consistency of the UCCSD ansatz can be maintained when the molecular orbitals localized to each monomer are used, but it can be broken when the molecular orbitals delocalized to the dimer are used in the UCCSD ansatz.

Since the QPE-based full-CI is often implemented using the Trotter decomposition of the time-evolution operator, it is important to verify whether or not the QPE-based full-CI with Trotter decomposition automatically satisfies the size consistency condition. It is known that the full-CI energy is invariant with the choice of the reference molecular orbitals, but it is unclear how the robustness of the QPE-based full-CI energy with respect to the Trotter error is affected by the choice of the molecular orbitals used for the wave function expansion.

In this work, we have performed numerical quantum circuit simulations of the QPE-based full-CI by using the localized and delocalized molecular orbitals with various Trotter decomposition conditions, focusing on the size consistency condition. The paper is organized as follows. Section II introduces the QPE-based full-CI method. Section III describes the target molecular system in this work and provides the numerical simulation conditions. We also discuss the acceleration of the numerical simulation of the QPE quantum circuit based on the sequential addition of ancillary qubits. Section IV gives results of the numerical simulations. The summary of this work is given in Section V.

II. THEORY

The QPE is a quantum algorithm for finding eigenvalues and corresponding eigenvectors of a unitary matrix U in polynomial time.^{29,30} In quantum chemical calculations, the QPE is performed using the time evolution operator as the unitary operator,

$$U = e^{-iHt}. \quad (2)$$

The Born–Oppenheimer approximation³¹ is usually adopted and the electronic Hamiltonian is used as H . In the second quantized formula, the electronic Hamiltonian H is written as

$$H = \sum_{pq} h_{pq} a_p^\dagger a_q + \frac{1}{2} \sum_{pqrs} g_{pqrs} a_p^\dagger a_q^\dagger a_s a_r. \quad (3)$$

Here, h_{pq} and g_{pqrs} are one- and two-electron integrals, respectively, and the indices p, q, r , and s run over spin orbitals in the active space.

The textbook implementation of the quantum circuit for the QPE³² is shown in FIG. 1, which contains L qubits for wave function storage and N ancillary qubits for eigenphase read-out. The QPE-based full-CI consists of five steps: (1) preparation of the approximate wave function of the target electronic state using a *Prep* circuit, (2) generation of quantum

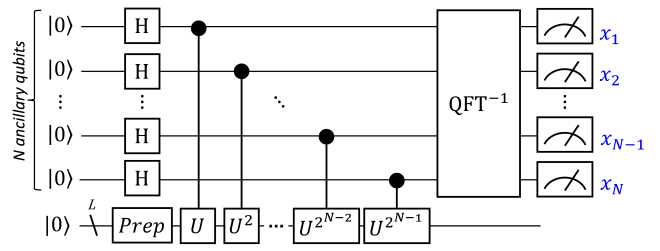


FIG. 1. The quantum circuit of the textbook implementation of QPE. x_1, x_2, \dots, x_N represent the measurement outcomes of ancillary qubits.

superposition states using Hadamard (H) gates, (3) controlled-time evolution operation, (4) inverse quantum Fourier transform, and (5) measurement of ancillary qubits. The bit string obtained from the measurement in step (5) corresponds to the fractional binary representation of the eigenphase $\phi = 0.x_1x_2\dots x_N$ in

$$e^{-iHt}|\Psi\rangle = e^{-iEt}|\Psi\rangle = e^{i2\pi\phi}|\Psi\rangle, \quad (4)$$

of one of the eigenstates. The probability of which eigenvalue is obtained is proportional to the overlap between the input wave function and the full-CI wave function.

In the quantum circuit implementation, the second quantized Hamiltonian in eq. (3) is transformed to a qubit Hamiltonian H_q ,

$$H_q = \sum_{j=1}^J w_j P_j, \quad (5)$$

using the fermion–qubit transformation techniques such as the Jordan–Wigner transformation (JWT)³³ and the Bravyi–Kitaev transformation (BKT)³⁴. Here, P_j is a tensor product of Pauli operators called as a Pauli strings, J is the number of Pauli strings, and w_j is the corresponding coefficient computed from h_{pq} and g_{pqrs} . Then, the time evolution operator in eq. (2) is implemented using the Trotter decomposition. The first-order and the second-order Trotter decompositions given as

$$e^{-iH_q t} = \left[\prod_{j=1}^J e^{-iw_j P_j t / M} \right]^M \quad (6)$$

and

$$e^{-iH_q t} = \left[\left(\prod_{j=1}^J e^{-iw_j P_j t / 2M} \right) \left(\prod_{j=J}^1 e^{-iw_j P_j t / 2M} \right) \right]^M, \quad (7)$$

respectively, are often used. Here, M is the number of Trotter slices. Besides the implementation based on the Trotter decomposition, approaches based on the truncated Taylor series^{35,36} and the qubitization³⁷ have also been proposed. The technique based on the qubitization shows better computational cost scaling compared to one based on Trotterization, but it requires additional ancillary qubits.³⁸ In this work, we focus on the Trotter decomposition-based approach.

It is well known that the full-CI energy is invariant to arbitrary unitary rotations of the molecular orbitals. For convenience, we focus on the HF canonical molecular orbitals

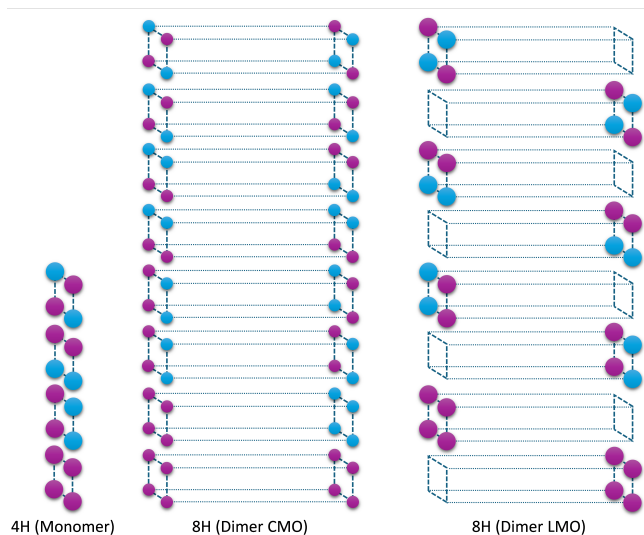


FIG. 2. The schematic illustrations of molecular orbitals being used. Intermonomer spacing is reduced for clarity. The lowest two and four orbitals for the monomer and the dimers, respectively, are doubly occupied in the HF wave function.

(CMO) and the localized molecular orbitals (LMO) as the two reference orbitals. By defining a unitary matrix V that interconverts the two different orbitals, the Hamiltonian matrices in the LMO and CMO bases are written as

$$H_{\text{LMO}} = V^\dagger H_{\text{CMO}} V. \quad (8)$$

Similarly, the time evolution operators can be written as

$$U_{\text{LMO}} = V^\dagger U_{\text{CMO}} V. \quad (9)$$

However, in the full-CI calculations using QPE with Trotter decomposition, the Trotterized time evolution operator U^{Trotter} does not necessary to satisfy the equality in eq. (9);

$$U_{\text{LMO}}^{\text{Trotter}} \neq V^\dagger U_{\text{CMO}}^{\text{Trotter}} V, \quad (10)$$

because the order of the Pauli strings in the Trotterized time evolution operator can depend on the molecular orbitals. We expect that the Pauli strings must be ordered in an appropriate way so that the Trotter error affects the monomer and the dimer in the same way to satisfy the size consistency condition.

III. COMPUTATIONAL CONDITIONS

In this work we consider a tetrahydrogen (4H) cluster in a square geometry with $R(\text{H-H}) = 1.0583 \text{ \AA}$ (2.0 Bohr) as the monomer, which is well known as a strongly correlated system.³⁹ The octahydrogen (8H) cluster as the dimer is constructed by placing two 4H clusters to form a cuboid, where the intermonomer distance is 100 \AA . The same system is also used in our previous work.²⁸ We used the STO-3G basis set and the active space contains all the molecular orbitals. The

size of the active space is (4e, 4o) and (8e, 8o) for 4H and 8H clusters, respectively. Here, (ke, lo) means that the active space contains k electrons and l molecular orbitals.

In the present study we used two different sets of molecular orbitals for the dimer calculations, the CMOs delocalized to the dimer under the D_{2h} point group and the LMOs under the C_{2v} point group. The schematic illustrations of the CMO and LMO are given in FIG. 2. These molecular orbitals are generated using the GAMESS-US software⁴⁰.

The conventional fermion-qubit transformations such as JWT and BKT require $2l$ of qubits to encode the wave function. In this work, we used the symmetry-conserving Bravyi-Kitaev transformation (SCBKT),⁴¹ which is able to reduce two qubits by specifying the number of spin- α and spin- β electrons. Thus, the number of qubits for the wave function encoding (L in FIG. 1) is 6 and 14 for 4H and 8H clusters, respectively.

In the QPE simulations, we set the time length of the time evolution operator in eq. (2) to $t = 1.0$, and we used 10 ancillary qubits to read out the eigenphase. As the input wave function of the QPE, we examined the full-CI and the HF wave functions, to see the state dependence of the Trotter error. For the implementation of the controlled-time evolution operator, we used both the first-order and the second-order Trotter decompositions with $M = 1, 2, 5$, and 10. The Trotter error depends on the order of the Pauli strings. Unless otherwise stated, we used the magnitude ordering, where the Pauli strings are applied in the descending order of the absolute value of the corresponding coefficient, $|w_j|$.⁴² All the simulations were performed using our original Python3 code developed with the OpenFermion,⁴³ Cirq,⁴⁴ and cuQuantum⁴⁵ libraries. The Trotter-free time evolution as the reference is also implemented using the `expm` function in the SciPy library.⁴⁶

The computational cost of the quantum circuit simulations of the QPE-based full-CI is very large, and the acceleration of the numerical simulation is very important to study sizable systems with larger number of ancillary qubits. In the QPE with N ancillary qubits, we have to perform the controlled- U operation $2^N - 1$ times, and this is the most time-consuming process. In this study, we reduce the simulation cost by performing the quantum circuit sequentially by adding ancillary qubits one by one. The schematic representation of the QPE quantum circuit simulation is shown in FIG. 3. In this strategy, the most time-consuming controlled- $U^{2^{N-1}}$ is simulated with $L + 1$ qubits in the first step (the leftmost dotted square in FIG. 3). Then we add an ancillary qubit to simulate controlled- $U^{2^{N-2}}$ with $L + 2$ qubits in the second step (the second dotted square from the left in FIG. 3). In this approach, the simulation time of the second step is of the same order as that of the first step. This is because the depth of the quantum circuit in the second step is about half of that of the first step, but the number of qubits in the simulation increases by one in the second step. The former reduces the simulation time to be half, but the latter makes the simulation time about twice as long, and these effects almost cancel each other out. The QPE simulations based on the implementation in FIG. 3 can accelerate the QPE simulation about $\mathcal{O}(2^N/N)$ from the naïve implementation in FIG. 1, which means an exponential speed

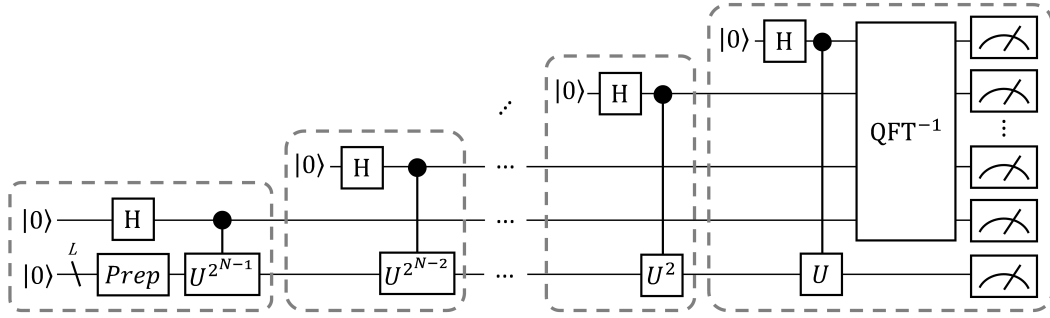


FIG. 3. The schematic illustration of the numerical simulations of the QPE-based full-CI with four ancillary qubits. Each step of the numerical simulation is specified by a dotted square.

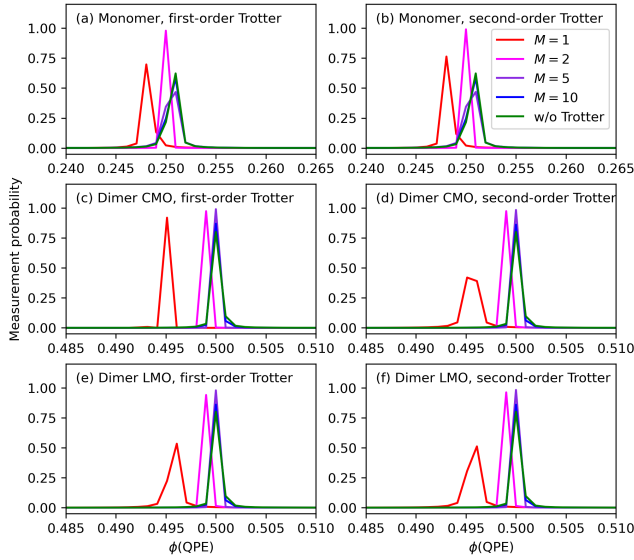


FIG. 4. The phase value versus measurement probability plot of the QPE simulation with the full-CI wave function as the input wave function. The magnitude ordering is used for the Trotter decomposition.

up of the numerical simulations.

IV. RESULTS

The phase value vs. measurement probability plots of the QPE-based full-CI as a function of the number of Trotter slices M are shown in FIG. 4 and 5, respectively, for the full-CI and the HF wave functions as the inputs. The peak obtained from the Trotterized time evolution operator is shifted from that calculated by the Trotter-free simulations for small M , but it converges to the Trotter-free one as M increases. Interestingly, both the CMO- and the LMO-based QPE simulations give the peak at almost the same position. The peak height becomes smaller when the HF wave function is used as the input because the overlap between the input and the full-CI wave functions is reduced, but the peak position is almost the same between the full-CI and HF inputs. Note that some

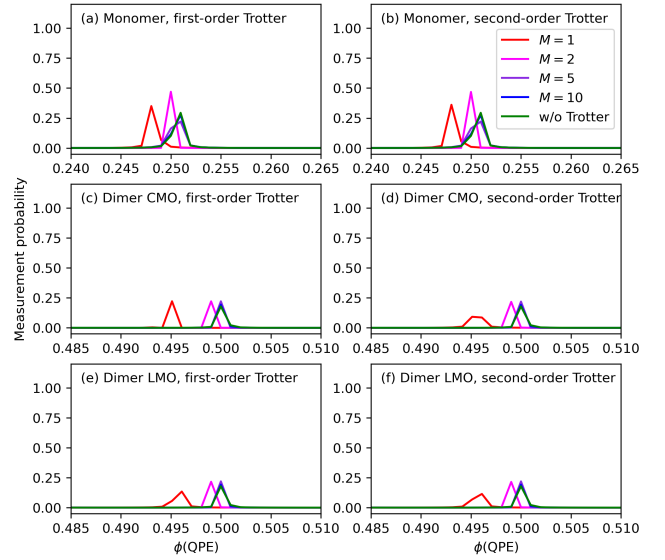


FIG. 5. The phase value versus measurement probability plot of the QPE simulation with the HF wave function as the input wave function. The magnitude ordering is used for the Trotter decomposition.

peaks have larger variance, due to the well-known “leakage problem” in the textbook implementation of the QPE.⁴⁷

To check the effect of the operator ordering in the Trotterized time evolution operator, we examined the lexicographic ordering in the Trotter decomposition. The results are shown in FIG. 6. As we expected, the trend of the Trotter error varied by changing the strategy of the operator ordering. In the dimer CMO calculations with the first-order Trotter decomposition, the calculated peak is already very close to the Trotter-free value even for $M = 1$, presumably due to fortuitous cancellation of errors (see FIG. 6(c)). However, for the first-order Trotter simulations with $M = 1$ in the dimer CMO, we observe an additional small peak around $\phi = 0.492$, even though the full-CI wave function is used as the input of the QPE. This is because the Trotterized time evolution operator is not equivalent to the original time evolution operator, and the full-CI wave function is no longer an eigenfunction of the Trotterized time evolution operator. The appearance of additional peaks

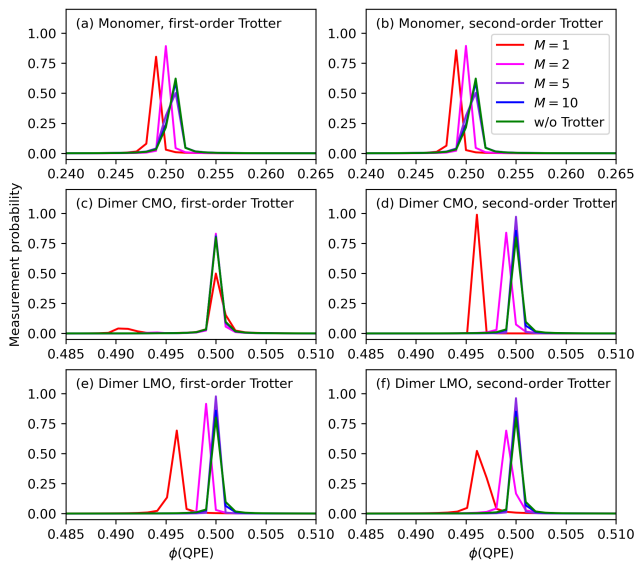


FIG. 6. The phase value versus measurement probability plot of the QPE simulation with the full-CI wave function as the input wave function. The lexicographic ordering is used for the Trotter decomposition.

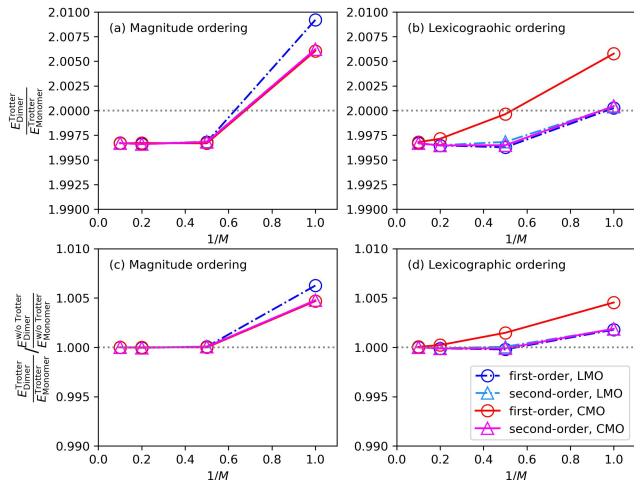


FIG. 7. The ratio of the total energies of the dimer and the monomer calculated using (a) the magnitude ordering and (b) the lexicographic ordering. The ratio values normalized by the Trotter-free simulation results are plotted in (c) and (d).

implies the large deviation of U^{Trotter} from U , and a more sophisticated treatment in the Trotter decomposition is desired.

The eigenphase value is evaluated by fitting the measurement probability plot with a Gaussian function. The ratio of the dimer and the monomer eigenenergies $E_{\text{Dimer}}/E_{\text{Monomer}}$ is calculated and plotted in FIG. 7(a) and (b) for the magnitude and the lexicographic orderings, respectively, as a function of $1/M$. In an ideal situation where the size consistency is strictly valid, the ratio $E_{\text{Dimer}}/E_{\text{Monomer}}$ should be two. In the present numerical simulations, however, the ratio deviates slightly from two even in the Trotter-free implementation,

probably due to rounding and leakage errors. In order to see the deviation of the $E_{\text{Dimer}}/E_{\text{Monomer}}$ values obtained from the Trotter decomposition-based simulation (denoted by ‘‘Trotter’’ in the superscript) from those of the Trotter-free simulations (denoted by ‘‘w/o Trotter’’ in the superscript), we plotted the $E_{\text{Dimer}}^{\text{Trotter}}/E_{\text{Monomer}}^{\text{Trotter}}$ normalized by the $E_{\text{Dimer}}^{\text{w/o Trotter}}/E_{\text{Monomer}}^{\text{w/o Trotter}}$ in FIG. 7(c) and (d) for the magnitude and the lexicographic orderings, respectively. In the present case, using $M = 1$ in the Trotter decomposition (Δt , the time length of a single Trotter slice, is 1.0) is insufficient to satisfy the size consistency condition, regardless of the method of operator ordering and the molecular orbitals used for the wave function expansion. By increasing the number of Trotter slices to $M = 2$, the size consistency condition is almost satisfied, except for the CMO with the first-order Trotter decomposition using the lexicographic ordering. Even in this case, the size consistency condition is systematically recovered by increasing the number of Trotter slices. Our numerical simulations revealed that the size consistency condition is not automatically violated by using the LMOs for the wave function expansion. However, the difference in the convergence behavior to the Trotter-free results with respect to the number of Trotter slices insists that the use of appropriate Trotter decomposition conditions, including the reference molecular orbitals, the order of the Trotter decomposition, and the operator ordering, are very important to satisfy the size consistency condition in the QPE-based full-CI calculations.

V. SUMMARY

A recent theoretical study on the VQE-UCCSD revealed that the size consistency can be broken by adopting the Trotter decomposition, when the molecular orbitals delocalized to the dimer are used.²⁸ In this study, we investigated the effect of the Trotter decomposition of the time evolution operator in the QPE-based full-CI calculations, focusing on the size consistency condition. Our numerical simulations of the 4H (monomer) and the 8H (dimer) clusters with the CMOs and the LMOs revealed that the eigenphase value obtained from the QPE is less affected by the choice of the molecular orbitals when the magnitude ordering is adopted, and the size consistency condition is almost maintained by setting the evolution time length of the single Trotter slice to be 0.5 or shorter. When the lexicographic ordering is used, the combination of the CMOs and the first-order Trotter decomposition is unsuitable from the viewpoint of the size consistency, but the size consistency condition can be systematically recovered by increasing the number of Trotter slices. The fact that the QPE-based full-CI can satisfy the size consistency condition when appropriate Trotter decomposition conditions are adopted is a good news for quantum chemical calculations on a quantum computer, especially when the large-scale quantum chemical calculations that are intractable on a classical computer become realistic. Combinations of the QPE with the fragmentation-based methods where the size consistency is a crucial condition, including divide-and-conquer (DC),⁴⁸ density matrix embedding theory (DMET),⁴⁹ and fragment

molecular orbital (FMO)⁵⁰ methods, seem to be a promising direction, and will be discussed in the forthcoming paper.

ACKNOWLEDGMENTS

The computation was carried out using the JHPCN Joint Research Projects (jh240001) on supercomputer ‘Flow’ at Information Technology Center, Nagoya University. K. Sugisaki acknowledges Takashi Abe, Yu-ya Ohnishi, Shu Kanno, and Yudai Suzuki for useful discussions. This work was supported by Quantum-LEAP Flagship Program (JPMXS0120319794) from Ministry of Education, Culture, Sports, Science and Technology (MEXT), Japan; Center of Innovations for Sustainable Quantum AI (JPMJPF2221) from Japan Science and Technology Agency (JST), Japan; and Grants-in-Aid for Scientific Research C (21K03407) and for Transformative Research Area B (23H03819) from Japan Society for the Promotion of Science (JSPS), Japan.

AUTHOR DECLARATIONS

Conflict of Interest

The author has no conflicts to disclose.

Author Contributions

Kenji Sugisaki: Conceptualization (Lead); Software (Lead); Investigation (Lead); Validation (Lead); Writing – original draft (Lead); Writing – review and editing (Lead)

DATA AVAILABILITY

The data that support the findings of this study are available from the corresponding author upon reasonable request.

REFERENCES

- A. Aspuru-Guzik, A. D. Dutoi, P. J. Love, and M. Head-Gordon, “Simulated quantum computation of molecular energies,” *Science* **309**, 1704–1707 (2005).
- L. Veis and J. Pittner, “Quantum computing applied to calculations of molecular energies: CH₂ benchmark,” *J. Chem. Phys.* **133**, 194106 (2010).
- M. Reiher, N. Wiebe, K. M. Svore, D. Wecker, and M. Troyer, “Elucidating reaction mechanisms on quantum computers,” *PNAS* **114**, 7555–7560 (2017).
- C. G. R. Babbush, D. W. Berry, N. Wiebe, J. McClean, A. Paler, A. Fowler, and H. Neven, “Encoding electronic spectra in quantum circuits with linear T complexity,” *Phys. Rev. X* **8**, 041015 (2018).
- J. Lee, D. W. Berry, C. Gidney, W. J. Huggins, J. R. McClean, N. Wiebe, and R. Babbush, “Even more efficient quantum computations of chemistry through tensor hypercontraction,” *PRX Quantum* **2**, 030305 (2021).
- N. P. Bauman, H. Liu, E. J. Bylaska, S. Krishnamoorthy, G. H. Low, C. E. Granade, N. Wiebe, A. Baker, B. Peng, M. Roetteler, and M. T. nd K. Kowalski, “Toward quantum computing for high-energy excited states in molecular systems: quantum phase estimations of core-level states,” *J. Chem. Theory Comput.* **17**, 201–210 (2021).
- I. H. Kim, Y.-H. Liu, S. Pallister, W. Pol, S. Roberts, and E. Lee, “Fault-tolerant resource estimate for quantum chemical simulations: case study on Li-ion battery electrolyte molecules,” *Phys. Rev. Res.* **4**, 023019 (2022).
- R. Izsak, C. Riplinger, N. S. Blunt, B. de Souza, N. Holzmann, O. Crawford, J. Camps, F. Neese, and P. Schopf, “Quantum computing in pharma: a multilayer embedding approach for near future applications,” *J. Comput. Chem.* **44**, 406–421 (2023).
- C. Kang, N. P. Bauman, S. Krishnamoorthy, and K. Kowalski, “Optimized quantum phase estimation for simulating electronic states in various energy regimes,” *J. Chem. Theory Comput.* **18**, 6567–6576 (2022).
- D. Hadler, V. S. Prasanna, V. Agarwal, and R. Maitra, “Iterative quantum phase estimation with variationally prepared reference state,” *Int. J. Quantum Chem.* **123**, e27021 (2022).
- P. A. M. Casares, R. Campos, and M. A. Martin-Delgado, “TFermion: a non-Clifford gate cost assessment library of quantum phase estimation algorithms for quantum chemistry,” *Quantum* **6**, 768 (2022).
- Y. Ino, M. Yonekawa, H. Yuzawa, Y. Minato, and K. Sugisaki, “Quantum phase estimations of benzene and its derivatives on GPGPU quantum simulators,” arXiv:2312.16375 (2023).
- M. Otten, B. Kang, D. Fedorov, A. Benali, S. Habib, Y. Alexeev, and S. K. Gray, “QREChem: quantum resource estimation software for chemistry applications,” arXiv:2404.16351 (2024).
- A. Roggero and J. Carlson, “Dynamical linear response quantum algorithm,” *Phys. Rev. C* **100**, 034610 (2019).
- K. Sugisaki, C. Sakai, K. Toyota, K. Sato, D. Shiomi, and T. Takui, “Bayesian phase difference estimation: a general quantum algorithm for the direct calculation of energy gaps,” *Phys. Chem. Chem. Phys.* **23**, 20152–20162 (2021).
- K. Sugisaki, “Projective measurement-based quantum phase difference estimation algorithm for the direct computation of eigenenergy differences on a quantum computer,” *J. Chem. Theory Comput.* **19**, 7617–7625 (2023).
- K. Kowalski, N. P. Bauman, G. H. Low, M. Roetteler, J. J. Rehr, and F. D. Vila, “Capturing many-body correlation effects with quantum and classical computing,” arXiv:2402.11418 (2024).
- R. Sakuma, S. Kanno, K. Sugisaki, T. Abe, and N. Yamamoto, “Entanglement-assisted phase estimation algorithm for calculating dynamical response functions,” arXiv:2404.19554 (2024).
- B. P. Lanyon, J. D. Whitfield, G. G. Gillett, M. E. Goggin, M. P. Almeida, I. Kassal, J. D. Biamonte, M. Mohseni, B. J. Powell, M. Barbieri, A. Aspuru-Guzik, and A. G. White, “Towards quantum chemistry on a quantum computer,” *Nat. Chem.* **2**, 106–111 (2010).
- J. Du, N. Xu, X. Peng, P. Wang, S. Wu, and D. Lu, “NMR implementation of a molecular hydrogen quantum simulation with adiabatic state preparation,” *Phys. Rev. Lett.* **104**, 030502 (2010).
- P. J. J. O’Malley, R. Babbush, I. D. Kivlichan, J. Romero, J. R. McClean, R. Barends, J. Kelly, P. Roushan, A. Tranter, N. Ding, B. Campbell, Y. Chen, Z. Chen, B. Chiaro, A. Dunsworth, A. G. Fowler, E. Jeffery, E. Lucero, A. Megrant, J. Y. Mutus, M. Neeley, C. Neill, C. Quintana, D. Sank, A. Vainsencher, J. Wenner, T. C. White, P. V. Coveney, P. J. Love, H. Neven, A. Aspuru-Guzik, and J. M. Martinis, “Scalable quantum simulation of molecular energies,” *Phys. Rev. X* **6**, 031007 (2016).
- K. Yamamoto, S. Duffield, Y. Kikuchi, and D. Muñoz Ramo, “Demonstrating Bayesian quantum phase estimation with quantum error detection,” *Phys. Rev. Res.* **6**, 013221 (2024).
- Y. Wang, F. Dolde, J. Biamonte, R. Babbush, V. Bergholm, S. Yang, I. Jakobi, P. Neumann, A. Aspuru-Guzik, J. D. Whitfield, and J. Wrachtrup, “Quantum simulation of helium hydride cation in a sild-state spin register,” *ACS Nano* **9**, 7769–7774 (2015).
- A. Peruzzo, J. McClean, P. Shadbolt, M.-H. Yung, X.-Q. Zhou, P. J. Love, A. Aspuru-Guzik, and J. L. O’Brien, “A variational eigenvalue solver on a photonic quantum processor,” *Nat. Comm.* **5**, 4213 (2014).
- J. Tilly, H. Chen, S. Cao, D. Picozzi, K. Setia, Y. Li, E. Grant, L. Wossnig, I. Runge, G. H. Booth, and J. Tennyson, “The variational quantum eigensolver: a review of methods and best practices,” *Phys. Rep.* **986**, 1–128 (2022).

- ²⁶A. Anand, P. Schleich, S. Alperin-Lea, P. W. K. Jensen, S. Sim, M. Diaz-Tinoco, J. S. Kottmann, M. Degroote, A. F. Izmaylov, and A. Aspuru-Guzik, "A quantum computing view on unitary coupled cluster theory," *Chem. Soc. Rev.* **51**, 1659–1684 (2022).
- ²⁷A. Szabo and N. S. Ostlund, *Modern Quantum Chemistry: Introduction to Advanced Electronic Structure Theory* (Dover Publication Inc., Minoela, NY, 1996).
- ²⁸K. Sugisaki, T. Nakano, and Y. Mochizuki, "Size-consistency and orbital-invariance issues revealed by VQE-UCCSD calculations with the FMO scheme," *J. Comput. Chem.* (2024), 10.1002/jcc.27438, published online.
- ²⁹A. Y. Kitaev, "Quantum measurements and the Abelian stabilizer problem," arXiv:quant-ph/9511026 (1995).
- ³⁰D. S. Abrams and S. Lloyd, "Quantum algorithm providing exponential speed increase for finding eigenvalues and eigenvectors," *Phys. Rev. Lett.* **83**, 5162–5165 (1999).
- ³¹M. Born and R. Oppenheimer, "Zur quantentheorie der molekeln," *Ann. Phys.* **389**, 457–484 (1927).
- ³²M. A. Nielsen and I. L. Chuang, *Quantum Computation and Quantum Information: 10th Anniversary Edition* (Cambridge University Press, Cambridge, UK, 2010).
- ³³P. Jordan and E. Wigner, "Über das paulische äquivalenzverbot," *Z. Phys.* **47**, 631–651 (1928).
- ³⁴J. T. Seeley, M. J. Richard, and P. J. Love, "The Bravyi–Kitaev transformation for quantum computation of electronic structure," *J. Chem. Phys.* **137**, 224109 (2012).
- ³⁵D. W. Berry, A. M. Childs, R. Cleve, R. Kothari, and R. S. Somma, "Simulating Hamiltonian dynamics with a truncated Taylor series," *Phys. Rev. Lett.* **114**, 090502 (2015).
- ³⁶A. Daskin and S. Kais, "A generalized circuit for the Hamiltonian dynamics through the truncated series," *Quantum Info. Proc.* **17**, 328 (2018).
- ³⁷G. H. Low and I. L. Chuang, "Hamiltonian simulation by qubitization," *Quantum* **3**, 163 (2019).
- ³⁸D. W. Berry, C. Gidney, M. Motta, J. R. McClean, and R. Babbush, "Qubitization of arbitrary basis quantum chemistry leveraging sparsity and low rank factorization," *Quantum* **3**, 208 (2019).
- ³⁹J. Paldus, P. Piecuch, L. Pylypow, and B. Jeziorski, "Application of Hilbert-space coupled-cluster theory to simple $(H_2)_2$ model systems: Planar models," *Phys. Rev. A* **47**, 2738–2782 (1993).
- ⁴⁰G. M. J. Barca, C. Bertoni, L. Carrington, D. Datta, N. De Silva, J. Emiliano Deustua, D. G. Fedorov, J. R. Gour, A. O. Gunina, E. Guidez, T. Harville, S. Irle, J. Ivanic, K. Kowalski, S. S. Leang, H. Li, W. Li, J. J. Lutz, I. Magoulas, J. Mato, V. Mironov, H. Nakata, B. Q. Pham, P. Piecuch, D. Poole, S. R. Pruitt, A. P. Rendell, L. B. Roskop, K. Ruedenberg, T. Sattasathuchana, M. W. Schmidt, J. Shen, L. Slipchenko, M. Sosonkina, V. Sundriyal, A. Tiwari, J. L. Galvez Vallejo, B. Westheimer, M. Wloch, P. Xu, F. Zahariev, and M. S. Gordon, "Recent developments in the general atomic and molecular electronic structure system," *J. Chem. Phys.* **152**, 154102 (2020).
- ⁴¹S. Bravyi, J. M. Gambetta, A. Mezzacapo, and K. Temme, "Tapering off qubits to simulate fermionic Hamiltonians," arXiv:1701.08213 (2017).
- ⁴²A. Tranter, P. J. Love, F. Mintert, and P. V. Coveney, "A comparison of the Bravyi–Kitaev and Jordan–Wigner transformations for the quantum simulation of quantum chemistry," *J. Chem. Theory Comput.* **14**, 5617–5630 (2018).
- ⁴³J. R. McClean, N. C. Rubin, K. J. Sung, I. D. Kivlichan, X. Bonet-Monroig, Y. Cao, C. Dai, E. Schuyler Fried, C. Gidney, B. Gimby, P. Gokhale, T. Häner, T. Hardikar, V. Havlíček, O. Higgott, C. Huang, J. Izaac, Z. Jiang, X. Liu, S. McArdle, M. Neeley, T. O’Brien, B. O’Gorman, I. Ozfidan, M. D. Radin, J. Romero, N. P. D. Sawaya, B. Senjean, K. Setia, S. Sim, D. S. Steiger, M. Staudtner, Q. Sun, W. Sun, D. Wang, F. Zhang, and R. Babbush, "OpenFermion: the electronic structure package for quantum computers," *Quantum Sci. Technol.* **5**, 034014 (2020).
- ⁴⁴Cirq Developers, "Cirq (v1.2.0)," Zenodo (2022).
- ⁴⁵H. Bayraktar, A. Charara, D. Clark, S. Cohen, T. Costa, Y.-L. L. Fang, Y. Gao, J. Guan, J. Gunnels, A. Haidar, A. Hehn, M. Hohnerbach, M. Jones, T. Lubowe, D. Lyakh, S. Morino, P. Springer, S. Stanwyck, I. Terentyev, S. Varadhan, J. Wong, and T. Yamaguchi, "cuQuantum SDK: A high-performance library for accelerating quantum science," arXiv:2308.01999 (2023).
- ⁴⁶P. Virtanen, R. Gommers, T. E. Oliphant, M. Haberland, T. Reddy, D. Cournapeau, E. Burovski, P. Peterson, W. Weckesser, J. Bright, S. J. van der Walt, M. Brett, J. Wilson, K. J. Millman, N. Mayorov, A. R. J. Nelson, E. Jones, R. Kern, E. Larson, C. J. Carey, Í. Polat, Y. Feng, E. W. Moore, J. VanderPlas, D. Laxalde, J. Perktold, R. Cimrman, I. Henriksen, E. A. Quintero, C. R. Harris, A. M. Archibald, A. H. Ribeiro, F. Pedregosa, P. van Mulbregt, and SciPy 1.0 Contributors, "SciPy 1.0: fundamental algorithms for scientific computing in Python," *Nat. Methods* **17**, 261–272 (2020).
- ⁴⁷Y. Xiong, S. X. Ng, G.-L. Long, and L. Hanzo, "Dual-frequency quantum phase estimation mitigates the spectral leakage of quantum algorithms," *IEEE Signal Proc. Lett.* **22**, 1222–1226 (2022).
- ⁴⁸W. Yang and T.-S. Lee, "A density-matrix divide-and-conquer approach for electronic structure calculations of large molecules," *J. Chem. Phys.* **103**, 5674–5678 (1995).
- ⁴⁹G. Knizia and G. K.-L. Chan, "Density matrix embedding: a simple alternative to dynamical mean-field theory," *Phys. Rev. Lett.* **109**, 186404 (2012).
- ⁵⁰K. Kitaura, E. Ikeo, T. Asada, T. Nakano, and M. Uebayasi, "Fragment molecular orbital method: an approximate computational method for large molecules," *Chem. Phys. Lett.* **313**, 701–706 (1999).